BNL--43465

DE90 003699

P R O P O S A L
for a Study of Laser Acceleration of Electrons using Micrograting Structures at the ATF (Phase I)

29 October 1989

W. Chen, J. Claus, R.C. Fernow[1], J. Fischer, J.C. Gallardo, H.G. Kirk, H. Kraner, Z. Li, R.B. Palmer, J. Rogers, T. Srinivasan-Rao, T. Tsang, S. Ulc, J. Veligdan & J. Warren
Brookhaven National Laboratory

I. Bigio , N. Kurnit & T. Shimada
Los Alamos National Laboratory

K.T. McDonald & D.P. Russell
Princeton University

X. Wang
U C L A

ABSTRACT

We propose to investigate new methods of particle acceleration using a short-pulse CO_2 laser as the power source and grating-like structures as accelerator "cavities"[1]. Phase I of this program is intended to demonstrate the principle of the method. We will focus the laser light to a 3 mm line on the surface of the microstructure. The structure is used to transform the electric field pattern of the incoming transversely polarized laser beam to a mode which has a component along the electron beam direction in the vicinity of the surface. With 6 mJ of laser energy and a 6 ps pulse length, the electric field in the spot will be around 1 GV/m. The electron beam from the Brookhaven Accelerator Test Facility (ATF) will be focused transversely within the few micron transverse dimension of the microstructure. The maximum expected acceleration for a 1 GV/m field and a 3 mm acceleration length is 3 MeV.

[1]Spokesman

1 Motivation

Many people believe that linear electron-positron colliders provide the only means for pursuing accelerator-based particle physics to higher center-of-mass regimes than those provided by the SSC generation of machines. This follows from the fact that the costs of circular machines increase like the energy squared, while the costs of linear colliders only grows linearly with energy. Although the constants of proportionality in these cost equations have a complicated dependence on the efficiency of available power sources, physical size, etc., it is clear that above some energy linear colliders will be more cost effective. It is also clear that, other things being equal, it is desirable to achieve the highest accelerating gradient possible. A 100 TeV collider which utilized accelerating cavities with a gradient of 1 GeV/m would have a total length of 200 km, which is only 2.4 times the circumference of the SSC. The same collider with conventional cavities giving 30 MeV/m gradient could just barely fit inside the United States.

Wavelength scaling

Studies of scaling laws from existing electron linacs suggest that there are advantages in choosing an operating wavelength shorter than the 10 cm currently used at SLAC[2]. The maximum achievable accelerating field depends directly on the peak electric field that can be maintained on the surface of the structure. Calculations, together with some experimental evidence, show that the maximum acceleration gradients increase with shorter pulse lengths or shorter wavelengths. In general the efficiency of a collider, expressed as the luminosity per unit power, will increase at shorter wavelength because of the smaller cavity volume which needs to be filled with electromagnetic energy.

There are also disadvantages to using shorter wavelengths[2]. The number of electrons per bunch decreases and this must be compensated for by some combination of increased source brightness, higher repetition rate, or smaller transverse dimensions at the interaction point. The trajectories of the bunches become less stable because of increased sensitivity to wakefield effects. Additional effects include tighter alignment and vibration tolerances, and more stringent requirements on damping rings. Thus there will be an optimum operating wavelength which depends on the development of many technologies and cannot be predicted with certainty at this time. Still, the consensus is that the optimum wavelength is shorter than 10 cm.

CO_2 laser as a power source

We have seen that to obtain high accelerating gradients it is desirable to have large electric fields and short pulses. In order to have efficient collider performance per unit power cost, it is desirable to have short wavelengths. The choice of existing power sources that can meet these requirements is limited. We propose to use a *short pulse CO_2 laser* as the power source. These lasers can produce enormous peak powers and we intend to investigate whether this property may be usefully employed for particle acceleration. Other possible applications include focusing, bunching, or fast kicking applications. Problems that must be solved in Phase I include producing a coherent laser wavefront, material damage limits, and synchronizing the short laser pulse with the arrival of the electron bunch. Equipment must be developed for monitoring the laser spatial distribution, intensity, and pulse length.

OPEN ACCELERATOR CAVITIES

It is believed to be very difficult or impossible to scale existing closed cavities to wavelengths smaller than about 1 mm. Besides the fabrication of the cavity itself, there is the problem of coupling radiation into it. The attenuation of the power in a travelling wave section will increase at shorter wavelengths. Thus the number of power feeds per unit length must be greater. Both these effects diminish the increased acceleration gradient that came from the shorter wavelength.

It is thus natural to consider abandoning conventional cavities and using instead so-called *open acceleration structures*. These are essentially acceleration sections built on top of or down into a planar surface. Open structures allow the incoming power to be supplied orthogonally and continuously along the electron beam axis. The result is that the peak power seen by the beam is constant along the axis of the linac and can be as large as the maximum surface field supported by the structure. The fabrication can be done using well developed etching and deposition techniques, while the radiation coupling can be achieved by focusing an external radiation beam onto the structure.

The characteristic dimensions of these structures scale with the free space wavelength of the power source, which is 10 μm for the experiments proposed here[3]. Techniques have been developed to reproducibly manufacture and measure the dimensional tolerances of these structures. However, it is important to keep in mind that any geometries which are developed can be scaled in size to another wavelength if other power sources are more promising than the CO_2 laser.

Useful open structures produce 3-dimensional fields which can be used for the acceleration of electrons. The required 3-dimensionality of the problem can be obtained by making the accelerating structure itself 3-dimensional or by bringing the incident radiation onto the structure in a non-symmetrical manner. The structure characteristics can only be approximated at present because adequate analytic tools and suitable computer programs are lacking[4]. The calculational efforts have been supplemented by microwave measurements of simple models of structures[5]. These measurements have been made at wavelengths around 3 cm. However, the size of the field probes used in the measurements and the wavelength dependence of material properties introduce some uncertainty in extrapolating the performance to 10 μm. The best probe at that wavelength is the electron beam itself.

We intend to examine both resonant and non-resonant structures. In both cases the incoming electromagnetic wave is linearly polarized. For non-resonant structures the electric field of the incident radiatior beam is directed along the particle beam axis. The electrons only absorb a small fraction of the available energy, the rest of which is reflected out of the system. Design and fabrication tolerances are much less critical than for resonant structures.

RESONANT OPEN STRUCTURES

Resonant structures contain elements that resonate electromagnetically with the incoming radiation. The particle beam is accelerated by the fields of these resonators rather than directly by the incoming radiation itself. The field strength in the resonator differs from that of the incoming beam by the Q factor. Frequency scaling laws and microwave modelling predict that this might still be on the order of 50–100 at 10 μm wavelength. Such resonant structures should behave similarly

to conventional ones, although their elements will be driven in parallel instead of series. One expects more efficient energy transfer from the source to the beam with a resonant structure. A well adjusted resonant structure should absorb nearly all the incoming radiation. The absorbed energy would then be distributed between the beam and dissipative losses in the structure.

An example of a resonant structure is the *colonnade*, shown in Fig. 1. This is a periodic, double row of identical cylinders sitting on top of a flat base plate. The structure behaves like an array of phased, dipole antennae. The structure can be prevented from strongly radiating by carefully controlling the position and sizes of the individual columns. Figure 2 shows another resonant structure known as a *foxhole*. This consists of a series of rectangular cavities with the top removed and connected by a narrow beam channel. Each cavity is individually coupled to the incoming radiation.

2 Structure fabrication

Simple non-resonant gratings may be purchased commercially. Fabrication techniques for more complex resonant structures have been developed at BNL[6]. A resonant grating designed for the Smith-Purcell experiment at the ATF can also be used for grating acceleration[7]. Considerable experimental work has been done to determine the feasibility of forming the structures by reactive ion etching. Several types of structures have been manufactured by etching fused silica in CHF_3 plasma or etching silicon with KOH/H_2O or ethylenediamine-pyrocatechol solutions. An example of a colonnade is shown in Fig. 3. Work is currently underway to make solid metal structures by etching in a layer of gold deposited over a copper base.

After the dimensions of a structure have been specified, the actual fabrication can be done within a few weeks. Considerable metrology must be done to determine adherence to specifications. Most of this analysis is performed using a high-resolution electron microscope that has been coupled to a line width, image analysis computer. Colonnade dimensions have been measured to be reproducible to 2% of the nominal size. After the initial set up period experimental measurements of a given structure at the ATF should only require a day or two. This relatively short turn around time will allow new concepts and parameter modifications to be tested relatively quickly.

3 Experimental arrangement

The experiment involves measuring the acceleration of electron bunches which have passed through the strong electric fields set up above open structures with a CO_2 laser. The electron beam bunch has an energy around 50 MeV, a momentum spread of ±0.2%, and a pulse length of about 2 mm (6 ps). It is focused to a transverse radius of 0.7 μm and a focal depth of ±1.5 mm at the center of the experimental stage. A pulse from the synchronized, cylindrically focused CO_2 laser beam is directed perpendicularly to the electron beam onto the center of the stage. The laser pulse sets up fields on the surface of the structure which perturb the beam either directly, or indirectly by first exciting the resonators. In cross section the focused light beam will extend about 5 mm along the electron beam axis and several wavelengths along the surface in the direction perpendicular to the beam. The

probing electron beam moves over the stage and the change in momentum is then analyzed in an imaging spectrometer.

ELECTRON BEAMLINE

The proposed ATF low intensity beamline to the experiment is shown in Fig. 4. The additional beamline components necessary for this experiment are three precision collimators, a final focus system, and a beam profile detector capable of measuring the beam size and divergence near the beam waist.

The beam leaving the linac enters an *emittance selection* section that ensures that the beam has the required small emittance[8]. In principle a beam of the proper dimensions can be produced with a sufficiently small spot at the photocathode. However, emittance growth can occur from fringe fields and higher order magnetic effects in the transport lines and linac. The section contains two precision collimators capable of closing to 100 μm. The collimators are separated by a phase advance of 90° in both transverse dimensions in order to get small emittances in both the x and y planes.

Following the emittance selection region there is an *achromatic transport line* to bring the beam to the final focus system. This section contains two dipoles. If necessary the momentum bite of the beam can be reduced to ±0.2% by placing another collimator at the point of maximum dispersion in this section.

The *final focus* system consists of six quadrupoles mounted on a rigid frame. It takes the nearly parallel horizontal spot coming through the precision collimator, rotates it by 90° in the phase space of both transverse dimensions, and delivers a 0.7 μm spot at the center of the accelerating structure. The depth of focus is ±1.5 mm.

A critical item in the ultimate success of this experiment is knowing the beam position at the target station, so the beam can be steered through the tiny few-micron channels in the structures. We propose to measure the beam position with micron resolution by using a silicon *microstrip detector.* A layout of one side of the detector chip is shown in Fig.5. The active strips are 1 micron wide and are separated from neighboring strips by 1 micron inactive regions. Each measuring plane would have 100 active strips 1 mm long. Strips for measuring the x position are etched on one side of the detector, while strips for measuring y are on the other side. The overall size of the silicon chip is 14 mm on a side. Each plane also contains two large *quadrant detectors* for "gross" position measurement. The relative signals in the four quadrants would be used to find the beam spot and steer it onto the microstrips. We propose to incorporate three of these detectors into the target box. Each detector would be remotely inserted into the beam where it would make a destructive measurement. In normal operation all of the detectors would be removed from the beam.

CO_2 LASER SYSTEM

A schematic of the laser system is given in Fig. 6 . The synchronization system for the YAG laser and the RF driving system begins with a 40.8 MHz master oscillator. The 40.8 MHz signal is used to directly drive the mode locked cw Nd:YAG laser. The 2856 MHz RF drive frequency is obtained by stepping up the master oscillator by a factor of 70.

We have chosen a cw Nd:YAG oscillator over a pulsed oscillator because commercial cw lasers have been demonstrated to have less than ±5 ps jitter. The mode locked pulses are 80 ps long and are produced at twice the drive frequency. The jitter between the YAG output pulses and the master oscillator signal will be kept below 1 ps using a commercial timing stabilizer[9,10].

The fiber is used to provide a linear frequency chirp. A single pulse is switched into and out of a regenerative YAG amplifier. A design using two Pockels cells for this purpose has been found to give reliable operation. Pulse compression down to 8–10 ps occurs automatically as the chirped pulse sweeps across the laser gain line. The amplified pulse enters two second harmonic generator (SHG) crystals to produce the 266 nm light for driving the e-gun photocathode. The repetition rate of the amplifier is limited to approximately 10 Hz. If higher repetition rate operation of the photocathode is desired for e-beam tuning, the system can be reconfigured to give a long pulse train with sufficient energy to drive the photocathode.

The CO_2 laser oscillator consists of an atmospheric pressure, transverse discharge laser with an intracavity low pressure discharge section to provide for single longitudinal mode operation. The oscillator produces ≈50 ns long pulses. The unconverted 1.06 μm light from the YAG laser is used to drive a two-stage (reflection plus transmission) germanium photoconductive switch. The first stage determines the leading edge of the output pulse while the second stage controls the trailing edge. Variable length pulses down to ≈6 ps can be obtained by adjusting the optical path length between the Ge plates.

The selected short pulse is then amplified in a multipass, high pressure CO_2 amplifier. The Los Alamos designed amplifier has a large gain length and large active volume. The unit has been modified for operation at 4 atm. The addition of an isotopic gas recirculator will provide sufficient bandwidth for amplification of a few picosecond CO_2 pulse.

Diagnostics will be designed to monitor the amplified CO_2 pulse length and energy. It would be desirable to be able to do this on a pulse-by-pulse basis. The optical beam will be transported up from the ATF laser table, across to the experimental area, and down through the beamline roof block. A remotely controlled positioning system will focus the CO_2 beam horizontally into the target box using an f/5 cylindrical mirror.

Experimental station

The electron beam and the laser pulse will converge on the accelerating structure inside the experimental station or *target box*. A schematic diagram of the important devices and movements in the box are shown in Fig. 7. This station, which contains six remotely controlled actuators and five monitors, requires a sophisticated design. We will attempt to maintain the box at as low a pressure as possible in order not to contaminate the electron beampipe vacuum and to minimize breakdown problems from gases adsorbed on the surfaces of the acceleration structures. A vacuum of 10^{-6} torr may be attainable.

In order to properly align the structure with the electron and the laser beams, the accelerating structure itself will sit on a remotely controlled stage with four degrees of freedom. The CO_2 laser beam must enter the box through an optically flat window that is transparent to 10 μm radiation. The box also contains the three

independently-insertable microstrip detectors for beam position monitoring, a pyroelectric detector array for measuring the intensity distribution at the CO_2 focus, and a Smith-Purcell monitor. The cylindrical focusing element for the CO_2 beamline is mounted just outside the window to the target box.

ANALYSIS SPECTROMETER

The analysis spectrometer sketched in Fig. 8 will be used to measure the change in momentum and deflection of the electron bunch after it passes over the structure[11]. The major components include a dipole magnet, quad triplet, 2-dimensional detector, scintillator telescope, and Faraday cup. The spectrometer has been laid out in such a way that it will be easy to quickly switch back and forth between the grating acceleration experiment and the non-linear Thomson scattering experiment. The X ray spectromemter will serve as a monitor when the grating acceleration experiment is running and the electron spectromenter will be a monitor when the Thomson scattering experiment is taking data.

A 20° bend, sector-shaped dipole magnet is used to momentum-analyze the electrons in the bunch. The quadrupoles determine the focal properties on the 2-dimensional detector. The preliminary magnet tune given in Table 1 uses point-to-point focusing in the bending plane and a point to roughly parallel focus in the other plane.

Table 1 Spectrometer magnetic design

	length [cm]	accumulated [cm]	strength [T/m]	[T]
AS	-	0.0		
D1	80.0	80.0		
BM	40.0	120.0		0.145
D2	50.0	170.0		
Q1	10.2	180.2	4.90	
D3	10.0	190.2		
Q2	20.4	210.6	3.80	
D4	10.0	220.6		
Q3	10.2	230.8	4.90	
D5	25.0	255.8		

This tune should produce a spot with a sigma of 50 μm in the bend plane and 500 μm in the non-bend plane. Since the laser enters the target box in the horizontal plane, the bending plane should be in the vertical direction so that the deflections generated by the interaction will be orthogonal to separations due to energy gain on the profile monitor. The scintillator telescope is used for rough timing and for beam alignment.

We are currently planning to use a 2-dimensional detector consisting of a phosphor screen profile monitor, image intensifier, and CCD camera[12]. This detector should have a spatial resolution of less than 100 μm and provide single electron detection efficiency. If for some reason the amount of light from the phosphor screen is insufficient, an alternate design using a bundle of scintillating fibers as the

radiator is also available[13]. The emitted light would be detected with a "night vision" type of CCD camera. The camera will be connected to a frame grabber so that the data will be available for computer analysis.

X RAY MONITOR

The laser field component perpendicular to the electron beam axis will accelerate the electrons transversely and cause them to emit X rays. This radiation can be used as a non-destructive diagnostic. The electrons see the laser light as a wiggler with about 300 periods of length equal to the wavelength of the laser, i.e. 10 μm. The emission is directed in the forward direction along the electron beam axis. We intend to use the X ray spectrometer from the non-linear Thomson scattering experiment as a monitor for the position and cross section of the beam in the vicinity of the structure[14].

SMITH-PURCELL MONITOR

Smith and Purcell discovered in 1953 that an electron beam skimming over the surface of a grating produces electromagnetic radiation[15]. The mechanism for acceleration over true gratings is the inverse of this effect. We intend to investigate the production of Smith-Purcell radiation from gratings, colonnades, and foxholes in an earlier experiment at the ATF. We will construct a beam-accelerating structure interaction monitor by placing a photomultiplier tube inside the target box at an angle corresponding to a measured peak for the production of visible radiation[7]. A second, external Smith-Purcell infrared detector will be used for empirically checking the correct angle of incidence of the laser onto the structures.

BEAM INTENSITY MONITOR

We propose to use a 50 MeV, low intensity Faraday cup just beyond the profile monitor for the analysis spectrometer to destructively monitor the intensity of electrons in each bunch.

DATA ACQUISITION SYSTEM

For convenience most detector development will use PC based systems and CAMAC instrumentation for signal readout. Later we intend to integrate the various detector systems into the ATF MicroVax-CAMAC data acquisition system by using an auxiliary crate controller. The PCs for the experiment may also connect directly to the MicroVax via Ethernet for file exchange.

4 Initial program

Our initial program will include a lengthy program of commissioning detectors, micron-level alignment, determining parameter limits, and system integration. After the equipment is fully debugged we will begin our studies of simple structures.

BEAM ALIGNMENT

We will use the three microstrip detectors in the target box for studying the focal properties and alignment of the electron beam. Our first task will be to commission the detectors and their readout system using the ATF beam. Important issues that must be addressed are instabilities in the beam position due to power supply fluctuations, thermal variations. vibrations, etc. Emittance growth due to magnetic field errors or wakefields must also be understood so that we can actually obtain

the required 0.7 μm spot. The mounting plate for the structures will be aligned with the electron beam position and direction using remotely controlled linear and rotary stages inside the target box.

BEAM–STRUCTURE INTERACTIONS

Once the electron beam is properly aligned with the structure, we can use the external Smith-Purcell detector to check the relative coupling of the beam with the structure. This is done without using the laser beam.

LASER FOCUS

It is essential that the CO_2 laser focus occurs at the location of the structure and that it is properly aligned with the electron beam direction. We will measure the relative energy distribution in the laser beam using the 1-dimensional pyroelectric detector array located in the target box. The focal length and orientation can be adjusted using remotely controlled actuators on the CO_2 focusing optics.

LASER–STRUCTURE INTERACTIONS

It is important to measure the maximum laser power that can be tolerated before a structure is damaged. This must be done for each type of structure. The fields in the laser pulse can be made to exceed 1 GV/m or 3 T in the focused spot, even in the absence of any structure. This may be large enough to induce field emission of electrons from metallic surface features[16]. Some measurements of this type will not require the electron beam.

BEAM–LASER INTERACTIONS

We can commission the X ray detector by sending the electron beam through the laser focus. Such measurements could be done with better efficiency by removing the structure and using higher laser power levels.

ACCELERATION EXPERIMENTS

A simple "2-dimensional" grating may be used as the first accelerating structure. The theory and predicted pattern in the analysis spectrometer are well understood for this structure. We would then begin a study of colonnades and foxholes, varying the shape and dimensions in order to achieve optimum performance.

5 Calculated results

Table 2 gives the basic parameters of the proof of principle experiment.

Table 2 Basic parameters

E_L	6	mJ	laser pulse energy
T_L	6	ps	laser pulse length
P_L	1	GW	laser peak power
$f_\#$	5		f-number of focusing optics
R_{INT}	53	μm	laser transverse focal radius
L_{INT}	3	mm	interaction length
σ_B	0.7	μm	electron transverse radius
P/A	0.31	TW/cm^2	power density at focus
G_{ACC}	1.5	GeV/m	accelerating gradient

The exact sensitivity of the experiment will depend on the final spectrometer layout and the resolution of the detector. In the phase I experiments the electron bunch length is long compared to a wavelength of CO_2 radiation. As a consequence all possible phase relations exist between individual electrons in the bunch and the radiation field.

TRUE GRATINGS

Let us first consider a 2-dimensional grating. If we arbitrarily say that 0° phase corresponds to maximum acceleration, then the fields above the grating are such that 90° phase corresponds to a deflection toward the grating surface, 180° corresponds to deceleration, and 270° corresponds to deflection away from the surface[3]. Intermediate phases involve combined accelerations and deflections. It is important to note that something happens to each electron. After passing through the dipole the accelerated and decelerated particles are bent apart in the direction perpendicular to the deflections. The focusing properties of the spectrometer are such that a circle-like pattern is formed on the detector.

Figure 9 shows the analysis screen viewed end-on for the cases when the electrons crossed the structure with the laser off and with the laser producing an accelerating field of 50 MV/m[17]. The small circles in the figure correspond to the response of the phosphor with 100 μm resolution to individual electron trajectories. The figure shows that by comparing the change in width of the pattern with the laser on and off, we should be able to measure total energy gains of 150 keV or more.

In figure 10 we show the detector hit pattern for an accelerating gradient of 500 MeV/m over the structure. The ring-like pattern is unmistakable (the magnification of the collection optics has been changed by a factor of 4 between figures 9 and 10). The radius of the ring is a measure of the strength of the fields that the particles saw while crossing over the grating. Note that the absolute location of the ring on the detector plane is not important.

COLONNADES AND FOXHOLES

The predicted pattern for a colonnade or foxhole is slightly more complicated because these structures posses a neutral axis. Particles travelling near the neutral axis are not deflected. This creates a band across the center of the ring pattern, as shown in Fig. 11.

By examining the patterns on the detector as the accelerating gradient on the structure is reduced, we have determined that the minimum detectable energy gain for the analysis spectrometer is around 150 keV. This corresponds to an accelerating gradient on the structure of 50 MeV/m and should be compared with the 1 GeV/m gradient that the structure may be capable of supporting.

Notes & References

[1] This proposal is based upon two similar ones which were first proposed for SLAC. The original SLAC proposal, *Laser Accelerator Test Beam*, 27 August 1985, called for using a 1 GeV beam extracted at section 10 of the SLAC linac. The second proposal, *Plan for studying Laser Acceleration*, 28 April 1986, was for a dedicated 50 MeV facility at End Station B.

[2] R.B. Palmer, *The interdependence of parameters for TeV linear colliders*, CAP-ATF Tech. Note 2, 21 September 1987; J. Claus, *Choice of parameters for linear colliders in multi-bunch mode*, in S. Turner (ed), New Developments in Particle Acceleration Techniques, CERN report 87-11, p. 161-80; J. Claus, *Energy efficiency and choice of parameters for linear colliders*, in Proc. of Seminar on New Techniques for Future Accelerators, Erice, 1986, published by Plenum Press, 1987.

[3] Calculations of acceleration based on "2-dimensional" gratings are given in R.B. Palmer, *A laser-driven grating linac*, Part. Acc. 11:81-90,1980.

[4] Three dimensional modeling is described in R.B. Palmer, *Open accelerating structures*, in S. Turner (ed), op.cit., p. 633-41; R.B. Palmer et al, *Report of Near Field Group*, in C. Joshi & T. Katsouleas(eds), Laser Acceleration of Particles, AIP Conf. Proc. No.130, 1985, p.234-52 and N. Kroll, *General features of the accelerating modes of open structures*, in C. Joshi, op. cit., p. 253-70; R.C.Fernow, *Properties of the colonnade accelerating structure*, note RCF-LA-8507, unpublished.

[5] M. Pickup, *A grating linac at microwave frequencies*, in C. Joshi, op. cit., p.281-95; R.B. Palmer & S. Giordano, *Preliminary results on open accelerating structures*, in C. Joshi, op.cit., p. 271-80.

[6] J. Warren, *Material considerations in the microfabrication of grating microstructures for use in a laser-powered linear accelerator*, Mat.Res.Soc.Sym.Proc. 76:129-33, 1987.

[7] R.C. Fernow, *Design of a grating for studying Smith-Purcell radiation and electron acceleration*, note BNL-42524, 1989.

[8] X. Wang & H.G. Kirk, *The Brookhaven Accelerator Test Facility: Laser Linac Beam Line*, unpublished (1989).

[9] A. Fisher, BNL, private communication.

[10] The inherent jitter and amplitude stability of a pulsed laser is likely to be considerably larger, and active stabilization cannot remove shot-to-shot flash lamp variations. Moreover, the fiber chirping pulse compression technique utilized for reducing the mode-locked pulse width is well suited to the cw YAG laser, while it cannot handle the pulse energies typically produced by pulsed YAG lasers.

[11] R.C. Fernow, *Updated 50 MeV spectrometer design*, note RCF-LA-8602, unpublished.

[12] D.P. Russell & K.T. McDonald, *A beam profile monitor for the BNL Accelerator Test Facility*, note DOE/ER/3072-52, unpublished.
[13] R.C. Fernow, *Scintillating fiber detector for the grating acceleration spectrometer*, note RCF-LA-8801, unpublished.
[14] The monitor envisioned here would be a simplified version of the one in K.T. McDonald et al, *Proposal for an experimental study of nonlinear Thomson scattering*, note DOE/ER/3072-39, unpublished.
[15] S. Smith & E. Purcell, *Visible light from localized surface charges moving across a grating*, Phys.Rev. 92:1069, 1953.
[16] Reproducible, sharp changes in measured parameters (e.g. the maximum energy gain) are likely to reflect the onset of field emission from parts of the structure surfaces, or perhaps other reversible changes in the behavior of the metal. Nonreproducible changes in measured parameters are likely to correlate with physical damage.
[17] Figures 9–11 correspond to an earlier magnetic design for the spectrometer. However, the essential features and sensitvities of these patterns can be made approximately the same for any reasonable designs.

Figure Captions

[1] Two possible configurations for a colonnade accelerating structure.
[2] The basic layout of a foxhole accelerating structure.
[3] Microphotograph of a colonnade structure etched on a silicon wafer. The white horizontal bar at the bottom indicates a distance of 1 micron.
[4] The ATF experimental floor showing the location of the grating acceleration experiment.
[5] Layout of the strips on one side of the microstrip beam position detector.
[6] Schematic of the CO_2 laser system.
[7] Schematic of the major components in the target box.
[8] Schematic of the analysis spectrometer layout.
[9] Calculated pattern of beam hits on the screen of the analysis spectrometer detector for a non-resonant grating accelerating structure. One pattern corresponds to the laser off condition (no field) while the other corresponds to a field of 50 MV/m over a 3 mm interaction region. Figures 9-11 have the energy dispersed direction along x.
[10] Calculated pattern of beam hits on the screen of the analysis spectrometer detector for a non-resonant grating accelerating structure. The laser on pattern corresponds to a field of 500 MV/m. Note that the magnification is a factor of 4 smaller than Fig. 9.
[11] Calculated pattern of beam hits on the screen of the analysis spectrometer detector for a foxhole accelerating structure. The laser on pattern corresponds to a field of 500 MV/m.

Colonnades

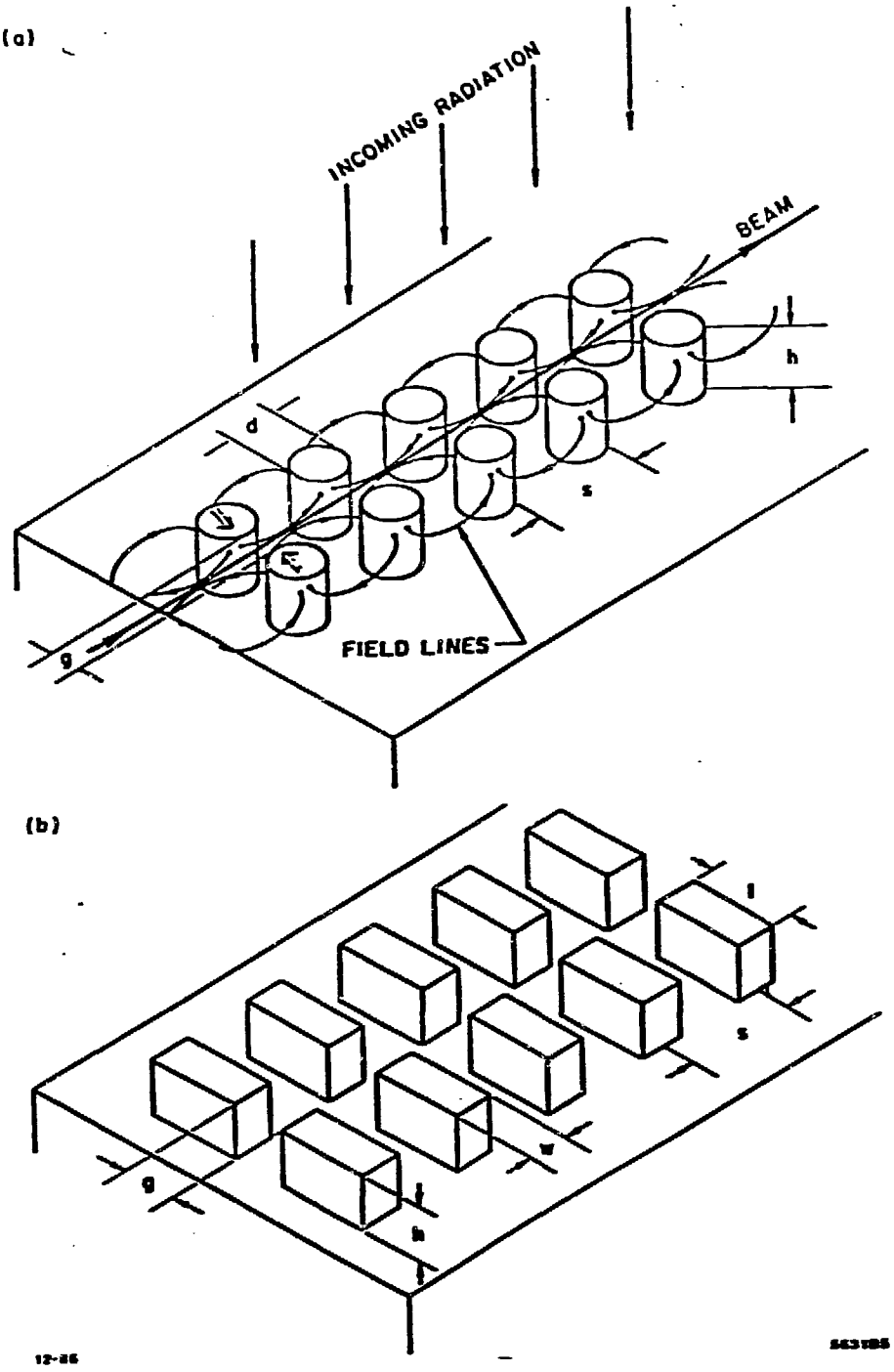

Fig. 1 Two alternative realizations of the collonade accelerating structure

Fig 2

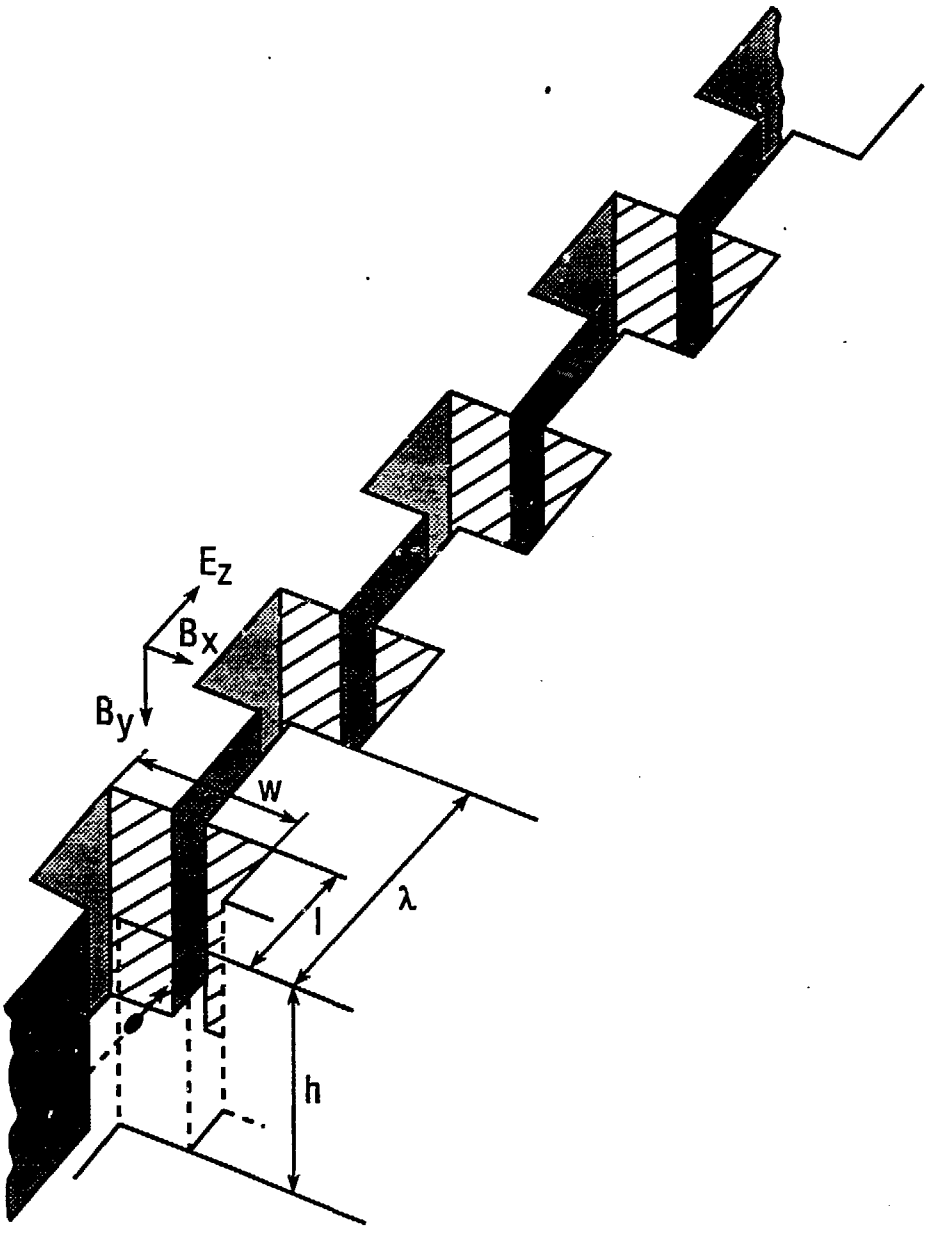

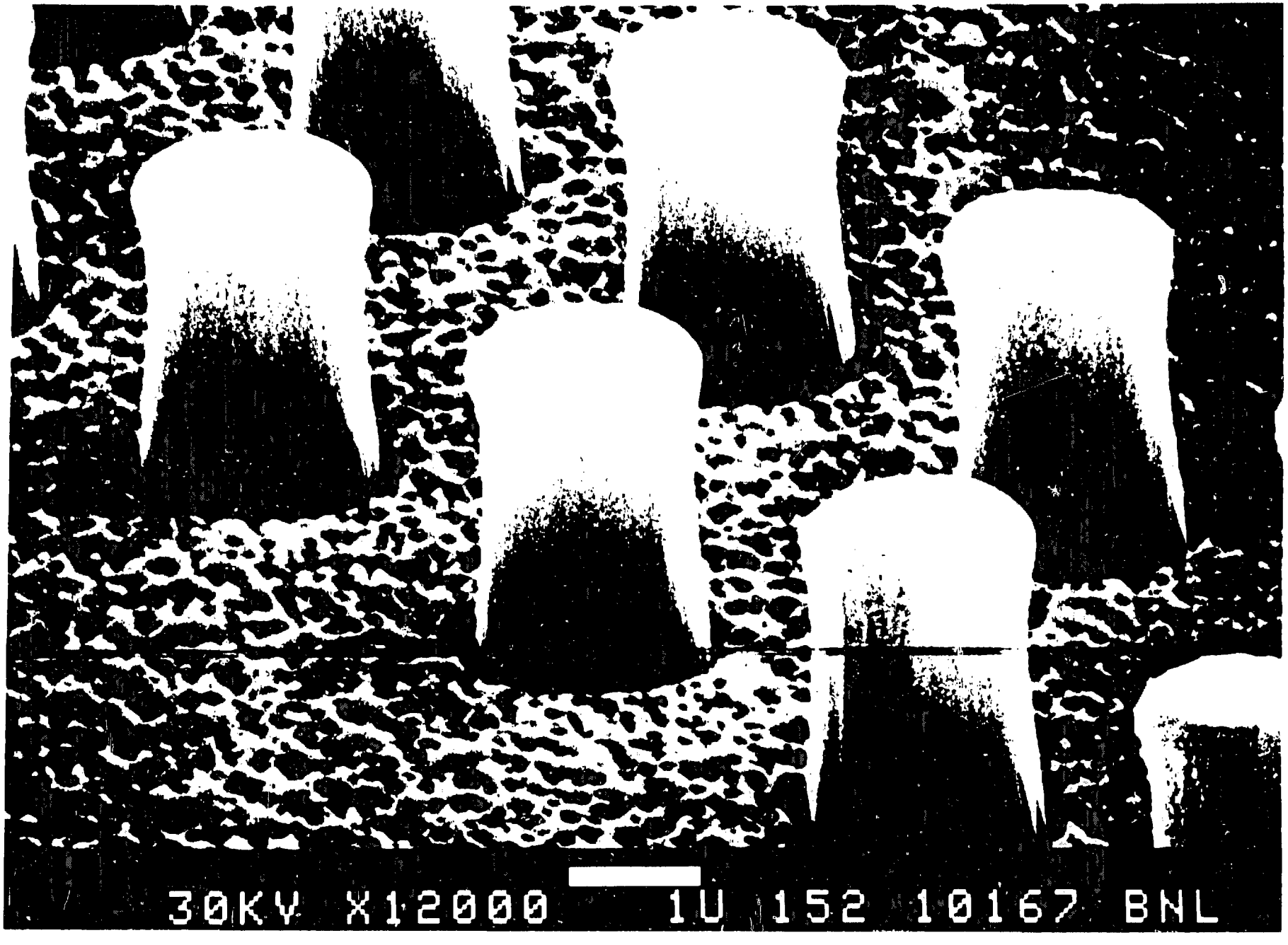

Fig. 3

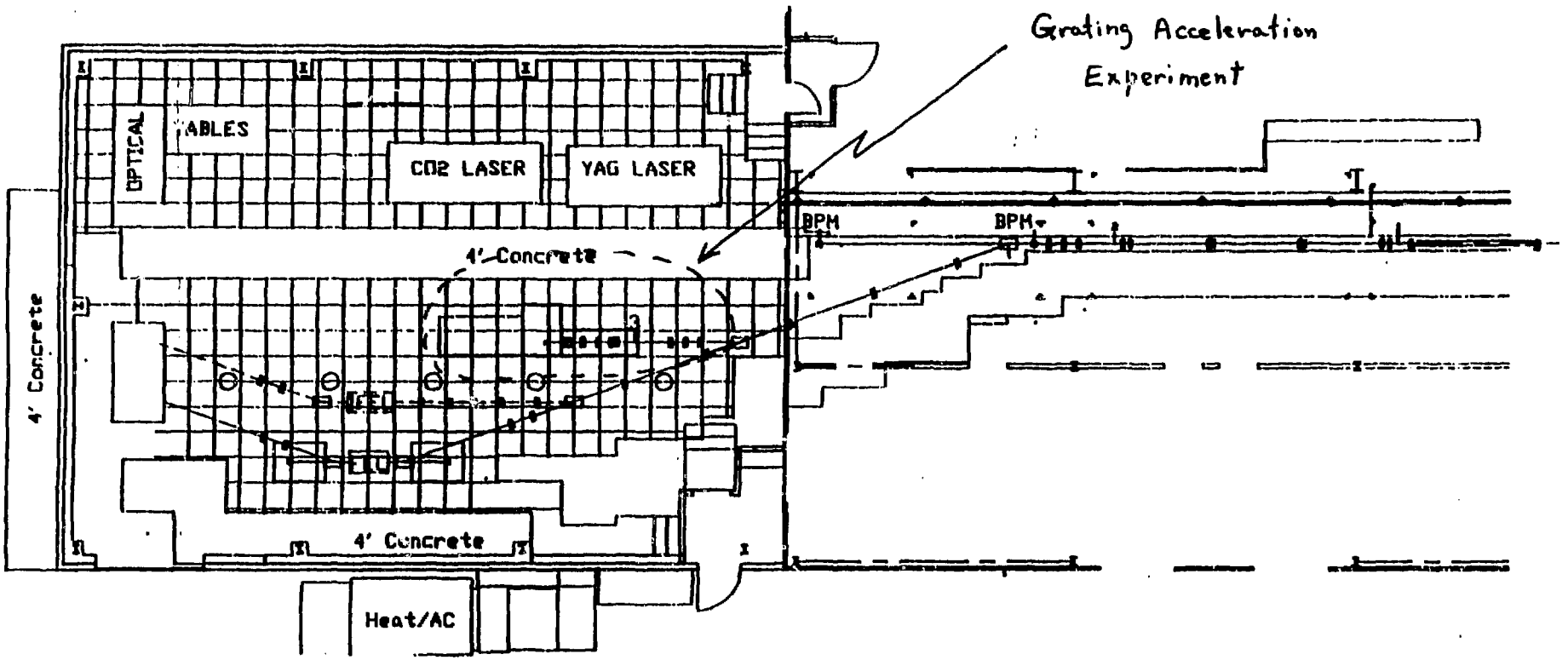

Fig.1 ATF experimental hall layout.

Fig. 5

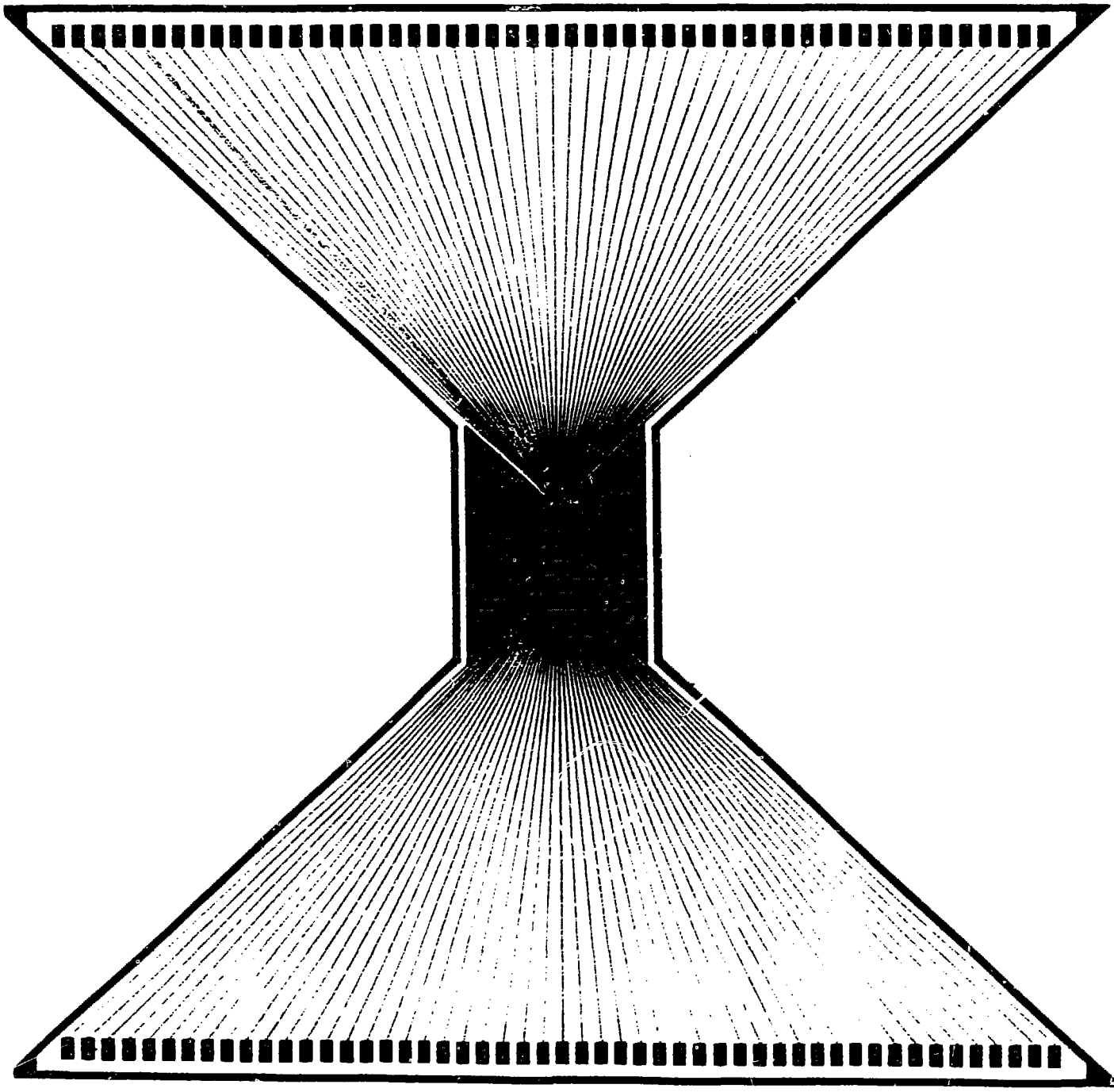

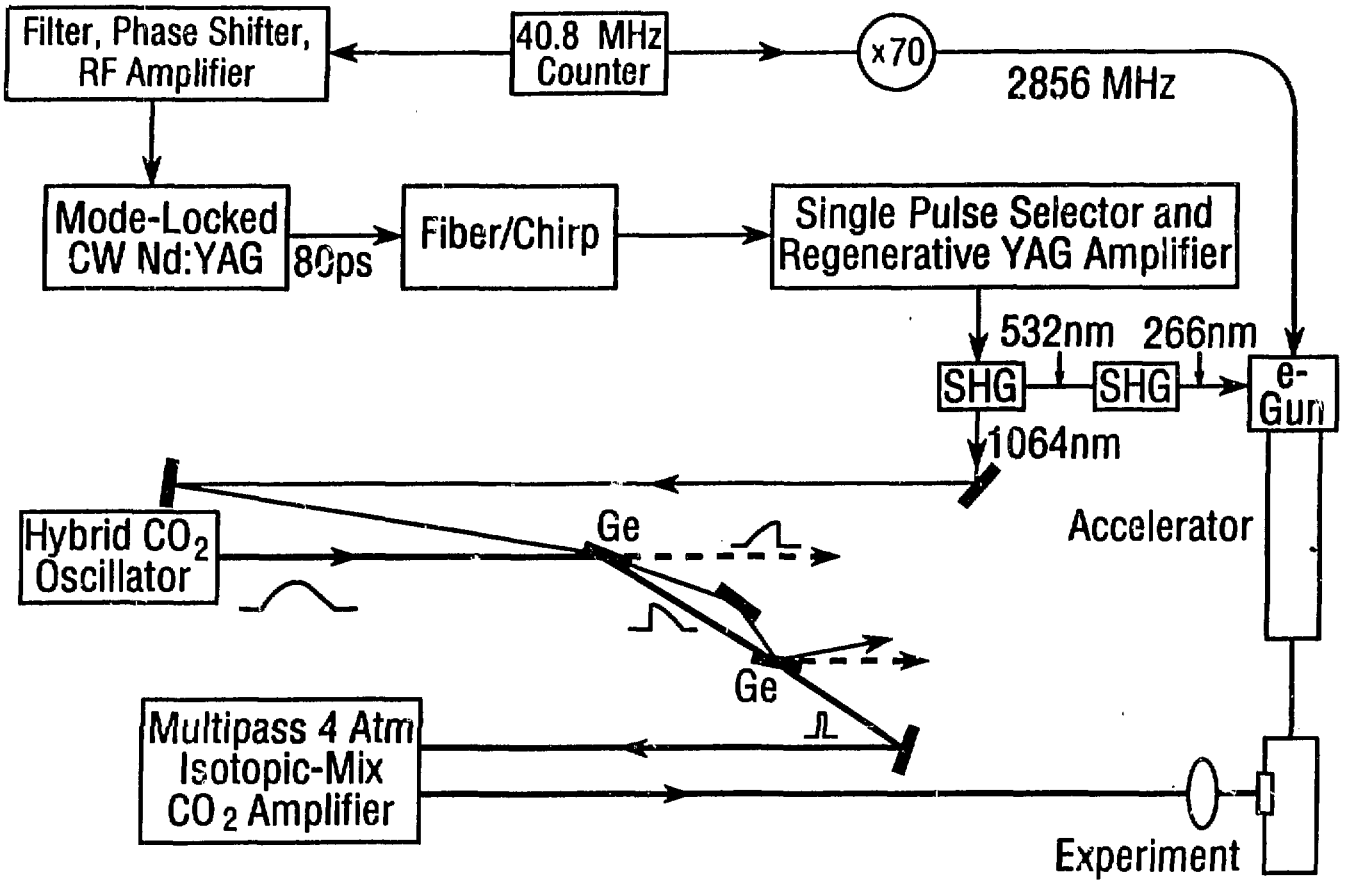
Filter, Phase Shifter, RF Amplifier
40.8 MHz Counter
x70
2856 MHz
Mode-Locked CW Nd:YAG
80ps
Fiber/Chirp
Single Pulse Selector and Regenerative YAG Amplifier
532nm
266nm
SHG
SHG
e-Gun
1064nm
Hybrid CO_2 Oscillator
Ge
Accelerator
Ge
Multipass 4 Atm Isotopic-Mix CO_2 Amplifier
Experiment

Fig 6

Fig. 7

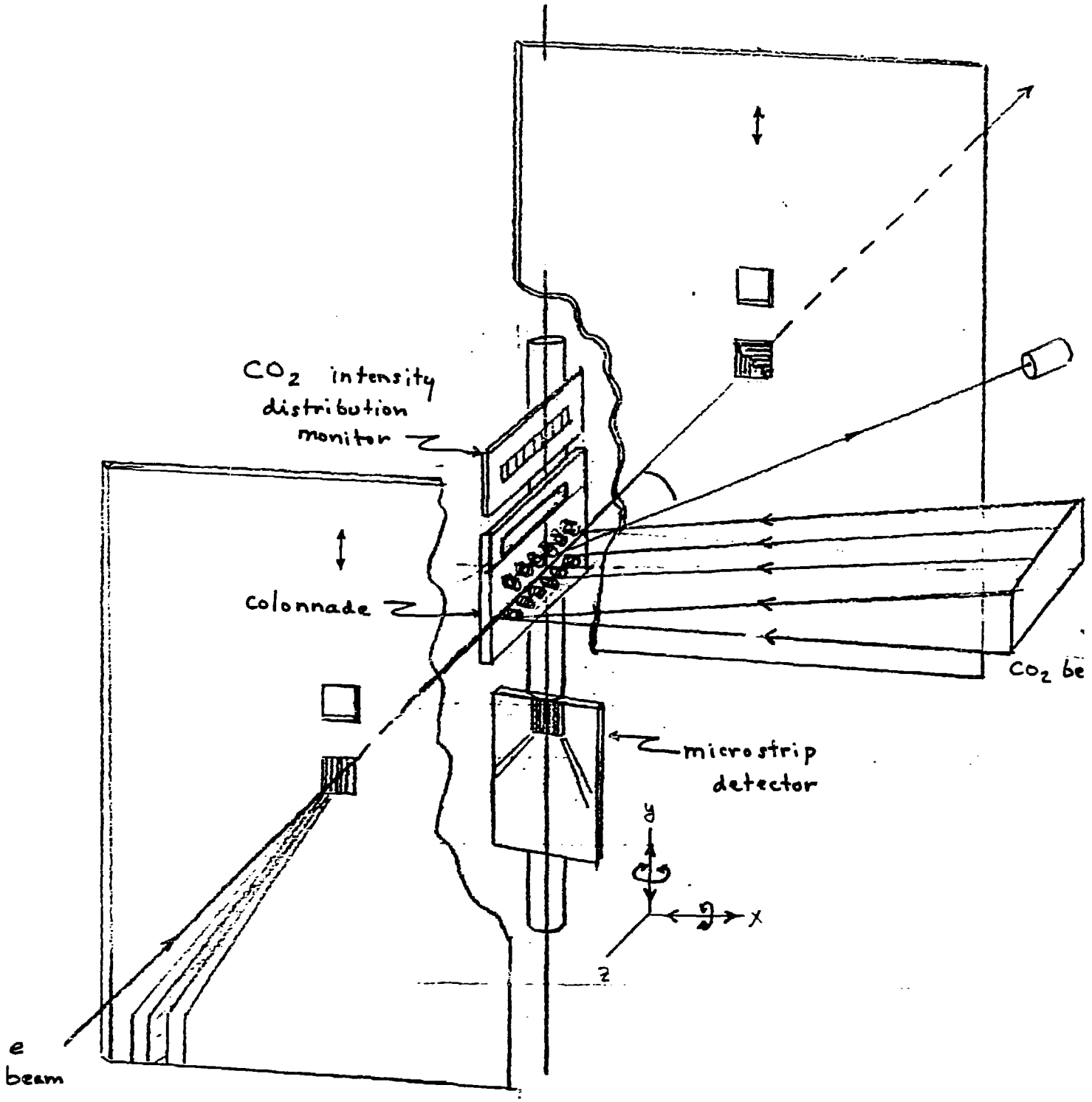
CO_2 intensity distribution monitor
Colonnade
microstrip detector
e beam
y
x
z

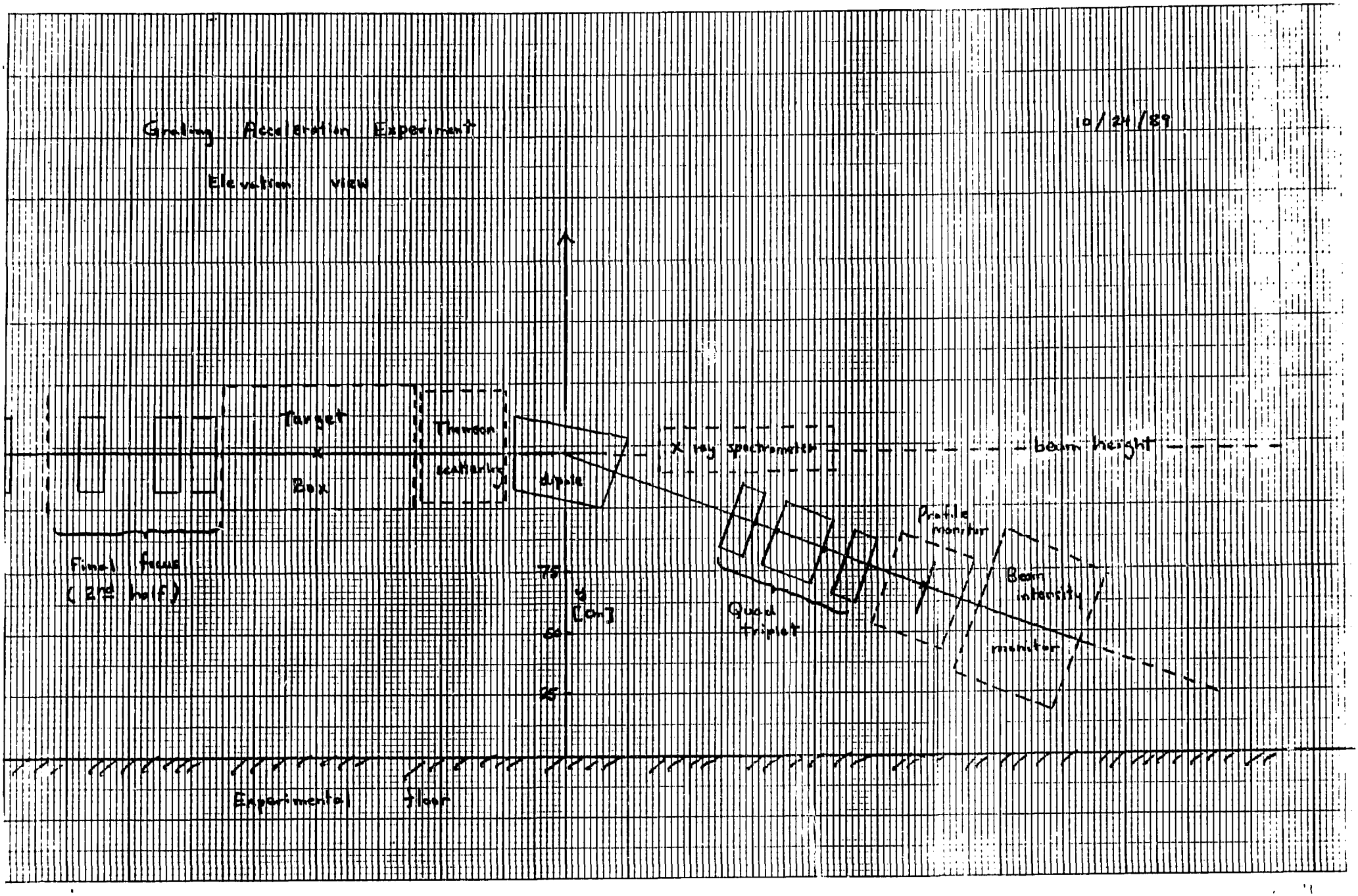

Fig 9

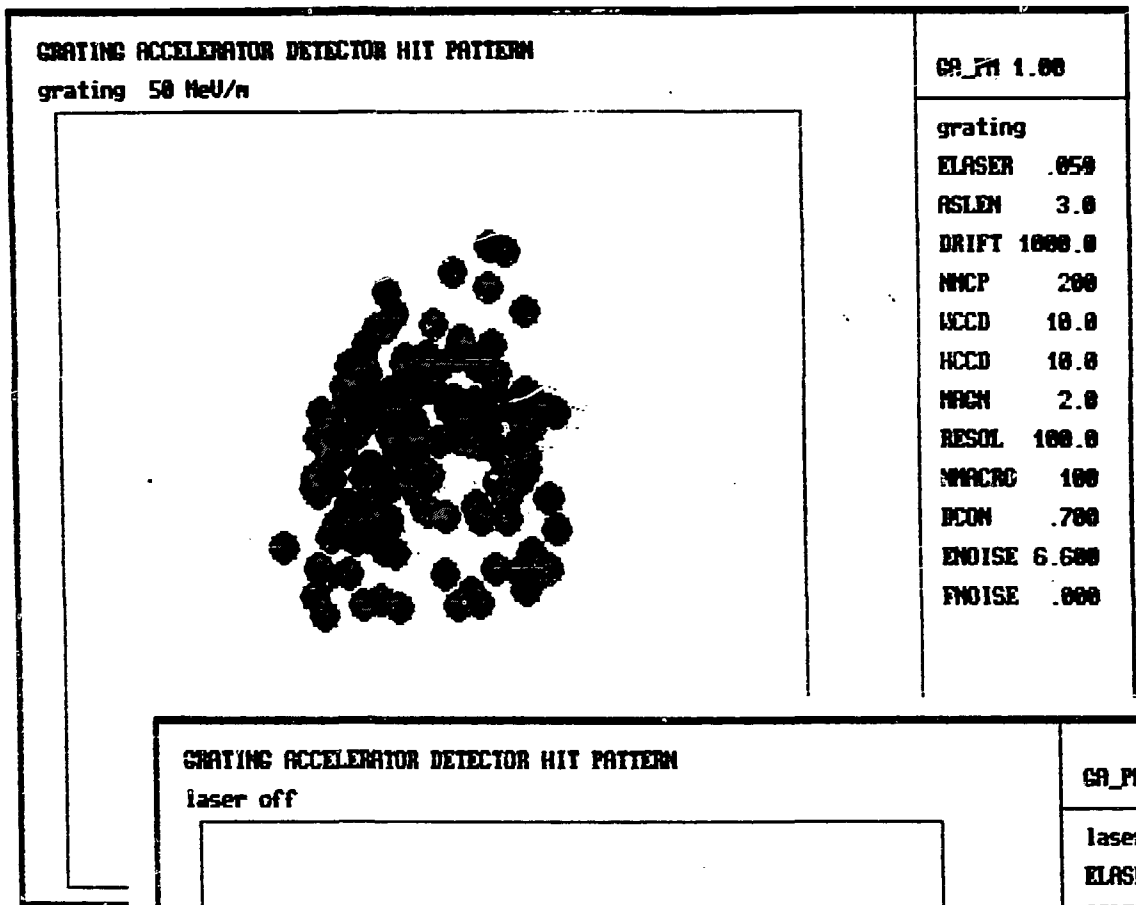
GRATING ACCELERATOR DETECTOR HIT PATTERN
grating 50 MeV/m
GA_PM 1.00
grating
ELASER .050
ASLEN 3.0
DRIFT 1000.0
NMCP 200
WCCD 10.0
HCCD 10.0
MAGN 2.0
RESOL 100.0
NMACRO 100
DCON .700
ENOISE 6.600
FNOISE .000

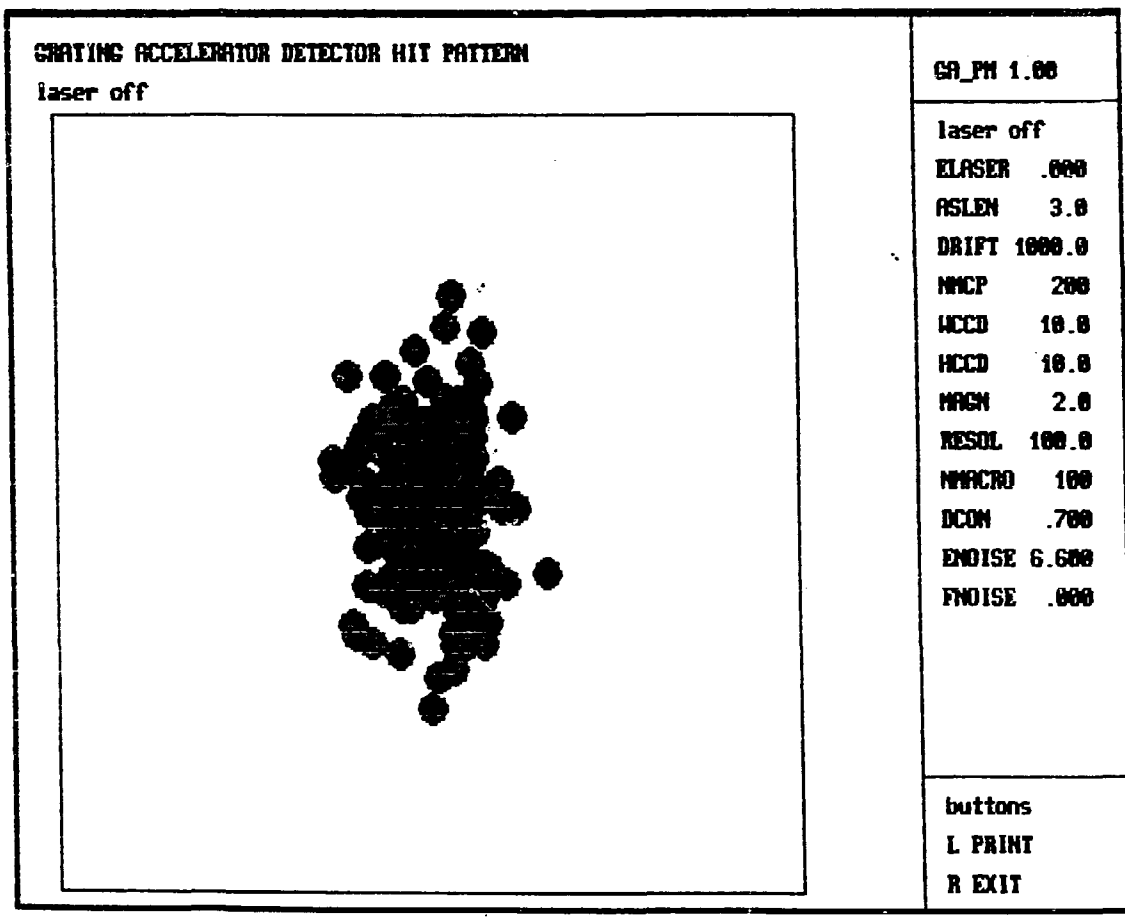
GRATING ACCELERATOR DETECTOR HIT PATTERN
laser off
GA_PM 1.00
laser off
ELASER .000
ASLEN 3.0
DRIFT 1000.0
NMCP 200
WCCD 10.0
HCCD 10.0
MAGN 2.0
RESOL 100.0
NMACRO 100
DCON .700
ENOISE 6.600
FNOISE .000
buttons
L PRINT
R EXIT

Fig. 10

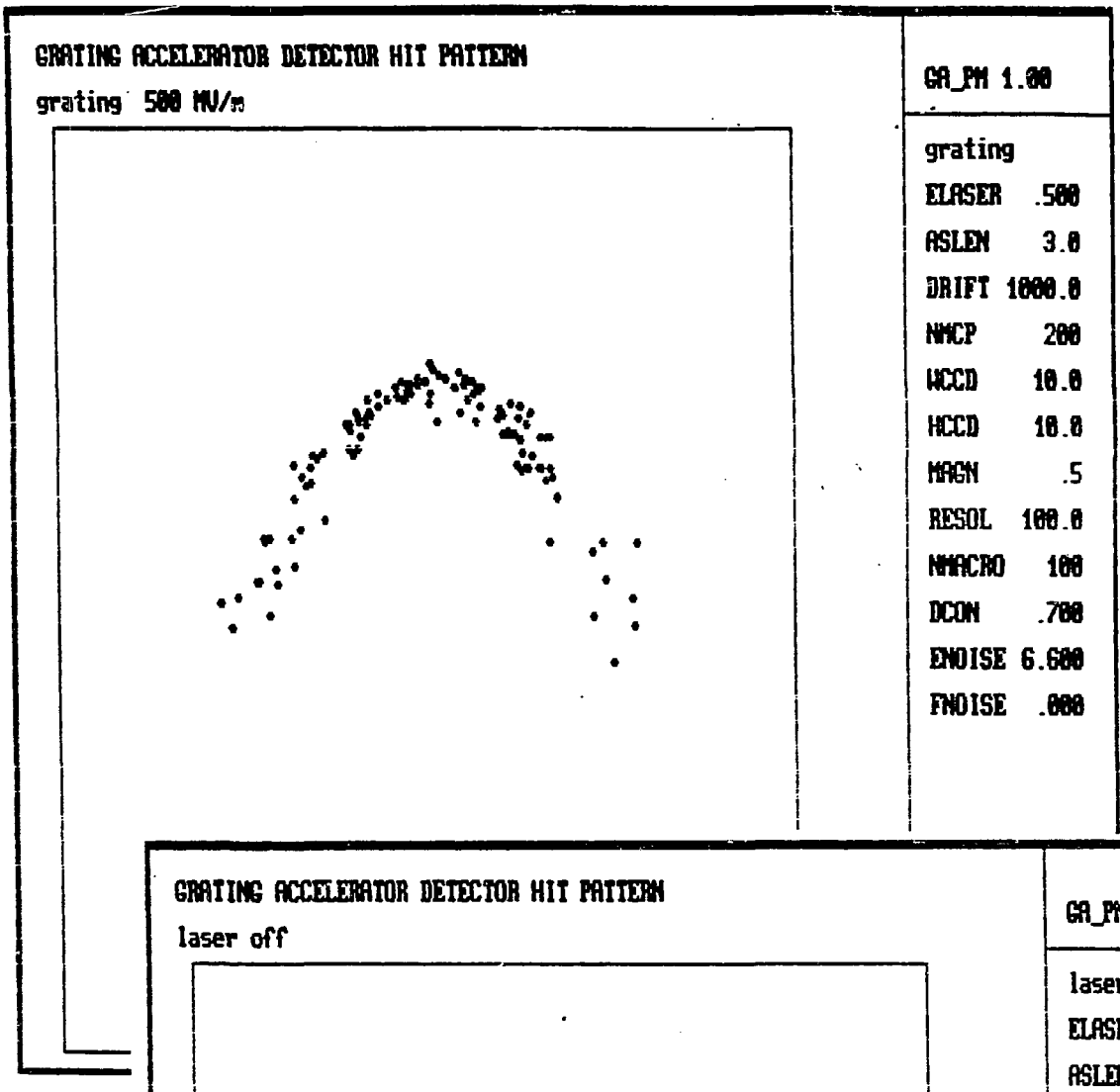
GRATING ACCELERATOR DETECTOR HIT PATTERN
grating 500 MV/m
GA_PM 1.00
grating
ELASER .500
ASLEN 3.0
DRIFT 1000.0
NMCP 200
WCCD 10.0
HCCD 10.0
MAGN .5
RESOL 100.0
NMACRO 100
DCON .700
ENOISE 6.600
FNOISE .000
GRATING ACCELERATOR DETECTOR HIT PATTERN
laser off
GA_PM 1.00
laser off
ELASER .000
ASLEN 3.0
DRIFT 1000.0
NMCP 200
WCCD 10.0
HCCD 10.0
MAGN .5
RESOL 100.0
NMACRO 100
DCON .700
ENOISE 6.600
FNOISE .000

Fig 11

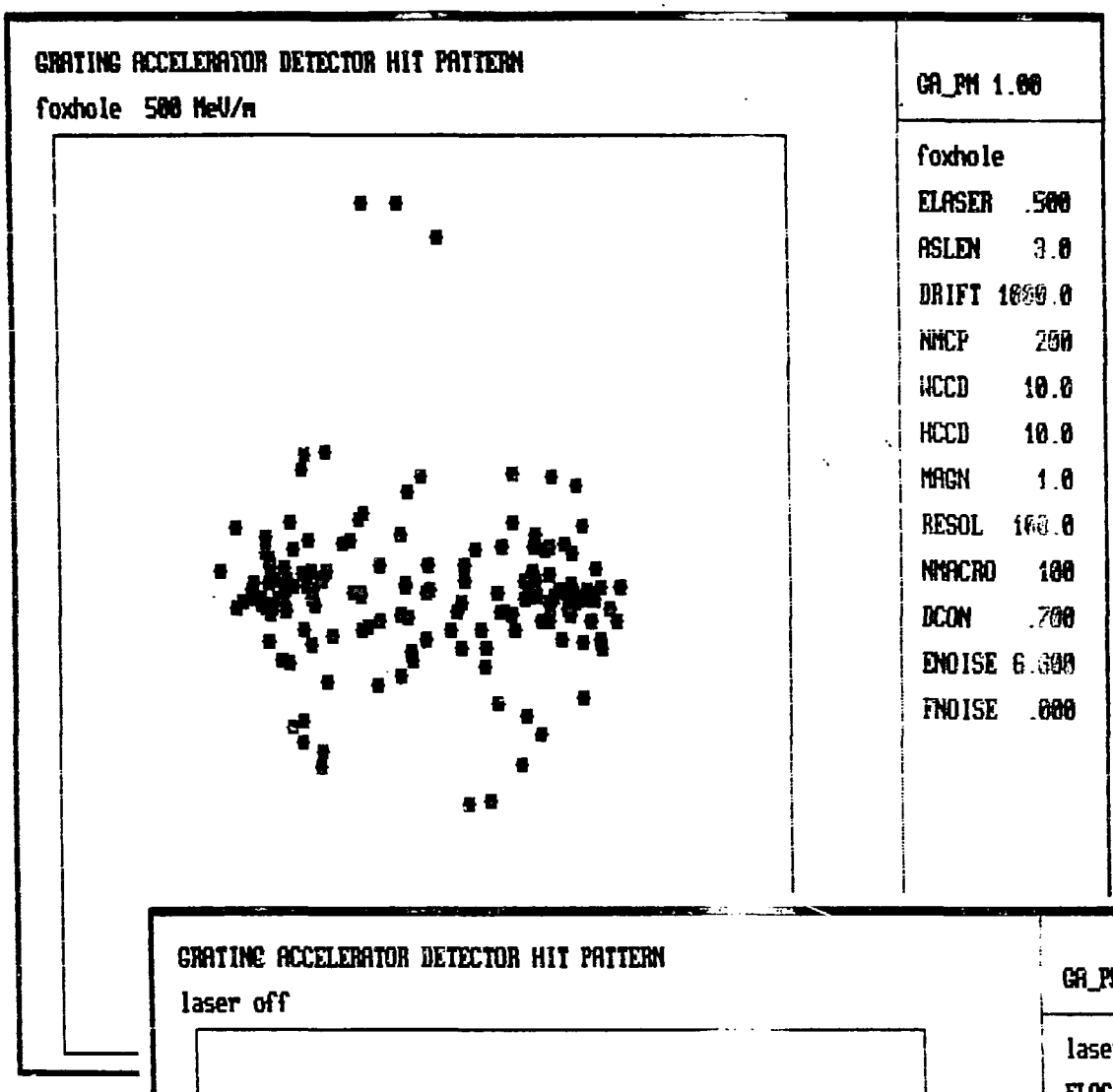
GRATING ACCELERATOR DETECTOR HIT PATTERN
foxhole 500 MeV/m
GA_PM 1.00
foxhole
ELASER .500
ASLEN 3.0
DRIFT 1000.0
NMCP 200
WCCD 10.0
HCCD 10.0
MAGN 1.0
RESOL 100.0
NMACRO 100
DCON .700
ENOISE 6.600
FNOISE .000

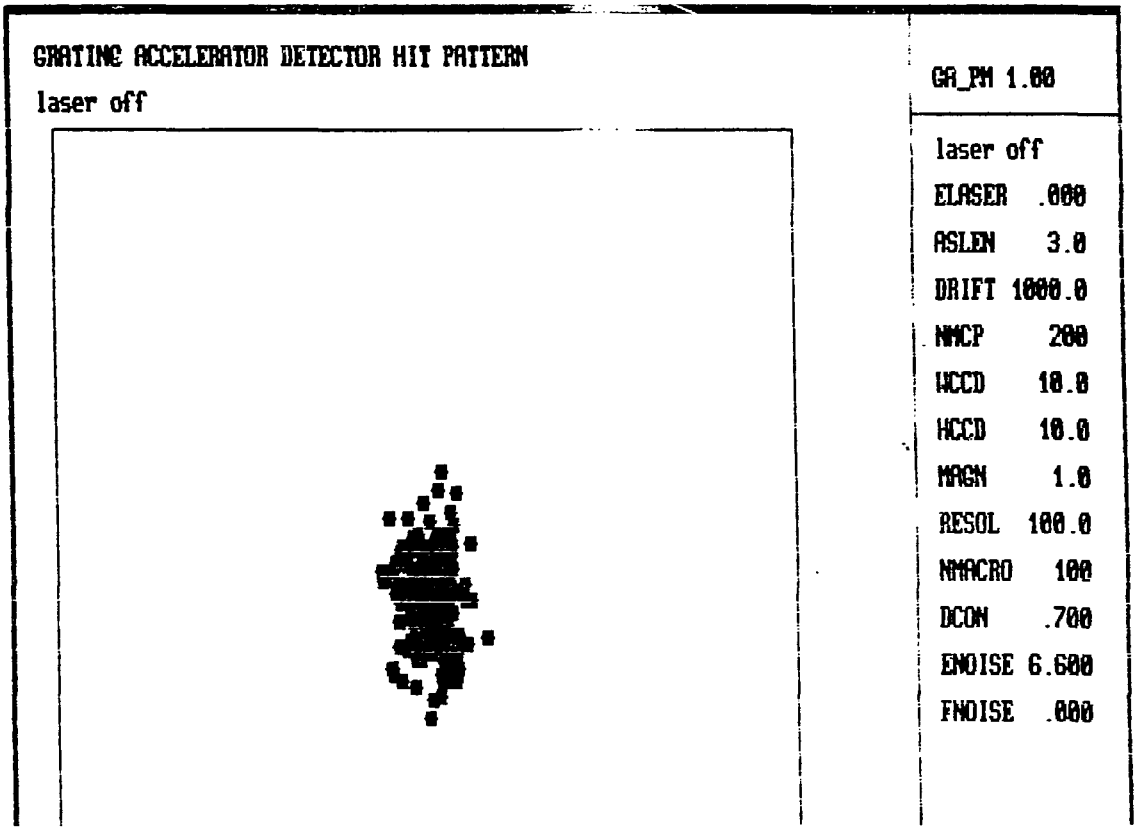
GRATING ACCELERATOR DETECTOR HIT PATTERN
laser off
GA_PM 1.00
laser off
ELASER .000
ASLEN 3.0
DRIFT 1000.0
NMCP 200
WCCD 10.0
HCCD 10.0
MAGN 1.0
RESOL 100.0
NMACRO 100
DCON .700
ENOISE 6.600
FNOISE .000